Surface plasmon resonance-enhanced refractive index sensing with cladding modes in photonic crystal fibers

O. Rusyakina,[1,2] T. Baghdasaryan,[1] K. Chah,[2] P. Mergo,[3] H. Thienpont,[1]
C. Caucheteur,[2] F. Berghmans,[1] and T. Geernaert[1]

[1] Brussels Photonics (B-PHOT), Vrije Universiteit Brussel and Flanders Make, Dept. of Applied Physics and Photonics, Pleinlaan 2, 1050 Brussels, Belgium
[2] Electromagnetism and Telecommunication Department, University of Mons, Boulevard Dolez 31,7000 Mons, Belgium
[3] Laboratory of Optical Fibres Technology, Institute of Chemical Sciences, Maria Curie Sklodowska University, Sklodowska Sq. 3, 20-031 Lublin, Poland

We demonstrate the excitation of cladding mode resonances in a hydrogen-loaded hexagonal lattice photonic crystal fiber (PCF) geometry by a straight Bragg grating in the fiber core region. These resonances feature effective indices close to the refractive index of water and demonstrate wavelength sensitivities of more than 40 nm/RIU for aqueous solutions in an extrinsic sensing configuration enhanced with a surface plasmon resonance mechanism. The sensitivity, figure of merit, and resolution of the reported PCF-based refractive index sensor are comparable to those of tilted Bragg gratings in step-index fibers, and better than those of extrinsic refractive index sensors in grating-equipped PCFs reported so far.

Introduction

Cladding modes guided in optical fibers have been widely considered for refractive index (RI) and bio-medical sensing. For example, the narrow resonances from tilted fiber Bragg gratings (TFBGs) in conventional step-index fibers allow *in situ* assessment of organic tissue with a catheter-based probe [1]. Cladding modes in photonic crystal fibers (PCF) have been studied as well [2,3]; yet, in those reports, the modes demonstrated low sensitivity to the surrounding RI. In this paper, we demonstrate the excitation of cladding mode resonances in a hexagonal lattice PCF geometry by a straight Bragg grating and their application for refractometry of aqueous solutions using a surface plasmon resonance (SPR) mechanism. Owing to the narrow spectral range occupied by the cladding modes, the proposed device may impact the challenge associated with multi-target biosensing with a single fiber probe by means of wavelength-multiplexed FBGs.

Grating inscription and setup for refractive index measurements

For our experiments, we considered a hexagonal lattice germanium doped PCF with six rings of air holes distanced at a pitch of $\Lambda = 2.5$ µm (air-filling factor is ~0.4) with a cladding diameter of 86 µm. A scanning electron microscope (SEM) image of the PCF microstructure is shown in the inset of Fig. 1. The fiber core region indicated with a light grey circle in the SEM image, is doped with 8.5 mol% germanium and has a diameter of the doped region of ~1 µm. A straight first order FBG was inscribed into a hydrogen-loaded PCF using a phase mask with a period of Λ_{PM} = 1082 nm and a 193 nm ArF excimer pulsed laser in a commercially available Noria FBG manufacturing station from NorthLab Photonics. The grating was written at an average laser power of 250 mW and approximate fluence at the photosensitive core of 2.8 kW/cm^2. For the spectral interrogation of the inscribed grating, the PCF was spliced to conventional single-mode pigtails from both sides.

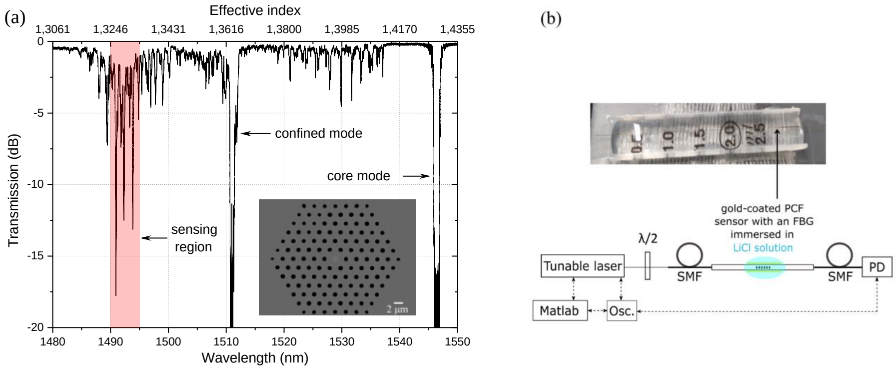

Fig. 1. **(a)** The transmission spectrum (in air) of a straight FBG inscribed into hexagonal lattice PCF (cross-section in the inset), with the red-colored region used for the SPR refractive index sensing. **(b)** The experimental setup for refractive index measurements with the PCF sensor.

We have previously shown that a complex interaction of the laser beam with the holey cladding during the FBG inscription results in a non-uniform intensity distribution and, therefore, a non-uniform refractive index modification over the PCF core region [4]. The mechanism of the cladding mode excitation with straight FBGs in PCFs can be attributed to this non-uniformity, similarly to point-by-point and eccentric gratings in step-index fibers [5]. In the transmission spectrum of the PCF with the inscribed FBG (Fig. 1a) we observe cladding mode excitation at several spectral positions with varying strengths of the resonances. This is in line with other reports of PCF grating transmission spectra [2,3]. The number of cladding modes in the PCF transmission spectrum is quite small when compared to the response of TFBGs in step-index fibers, which stems from the PCF microstructure that limits the number of modes existing in the fiber. The transmission spectrum in Fig. 1a shows two saturated resonances at 1546.8 nm (core mode) and at 1511 nm (confined cladding mode) which show no sensitivity to the surrounding refractive index (SRI). However, strong resonances located in the wavelength region 1490-1495 nm are sensitive to the external RI since their effective indices calculated from $\mathrm{n_{eff,clad}} = (2\,\lambda_{\mathrm{clad}}/\Lambda_{\mathrm{PM}}) - \mathrm{n_{core}}$ (where λ_{clad} is the resonance wavelength, and n_{core} the effective index of the core mode), are close to the refractive index of water. We are going to use these resonances for refractometry of aqueous solutions with an experimental setup shown schematically in Fig.1b. A tunable laser source was programmed to make a wavelength sweep between 1480 and 1550 nm. A half-wave plate (λ/2) placed after the laser source was used to rotate the linear polarization at the input of the PCF sensor. The transmitted power was recorded with a Thorlabs PDA20CS photodetector (PD). An oscilloscope (Osc.) synchronized the wavelength swept system and the PD output voltage to retrieve the transmission spectrum. Control of the setup and data collection were done using a MATLAB script. During the measurements, the PCF sample was fixed with the fiber clamps which minimized the effect of strain perturbations on the fiber.

Plasmonic-enhanced refractometry with the PCF sensor

To employ the surface plasmon excitation mechanism for signal enhancement, we deposited a layer of gold with a thickness of ~35 nm on the fiber surface in a sputter-coater chamber. To perform refractive index measurements, we prepared sixteen solutions of lithium chloride salt dissolved in distilled water at different concentrations with a step between the solutions of around 1×10^{-4} RIU. The RI of each solution was measured at 436.6 nm using a refractometer Abbemat MW and extrapolated to 1550 nm with the Sellmeier fit for distilled water (extrapolated RI values are indicated in Fig. 2b).

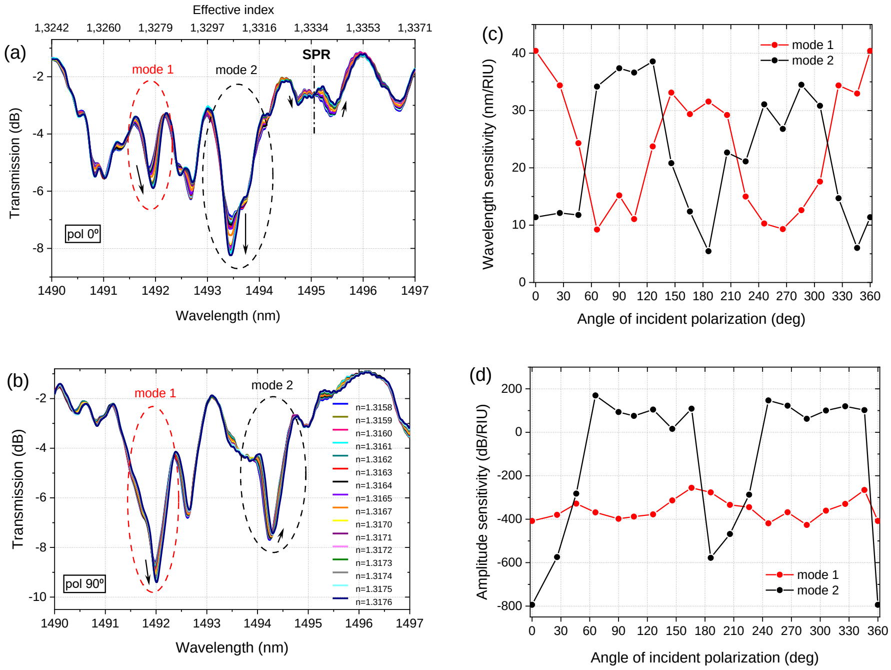

Fig. 2. **(a, b)** Transmission spectra of the gold-coated PCF sensor immersed in sixteen RI solutions for the polarization optimized for SPR excitation (a) and for the orthogonal polarization (b). The modes with the largest shift in wavelength and amplitude are indicated as mode 1 and 2, correspondingly. Black arrows indicate the direction of the wavelength and amplitude shifts with an increasing SRI. **(c, d)** Experimentally measured wavelength (c) and amplitude (d) sensitivity for different angles of the input polarization.

We rotated the input polarization with a half-wave plate to obtain the polarization state that resulted in the resonances with the largest spectral and intensity shifts as a function of an increasing SRI. Fig. 2 shows transmission spectra of the PCF sensor immersed in sixteen RI solutions for two orthogonal polarizations. The resonances that demonstrated the largest shifts in the wavelength and amplitude (mode 1 and mode 2) are indicated with dashed circles. The mode phase-matched to the plasmonic wave and, therefore, attenuated in the spectrum, is positioned at 1495.06 nm. Evolution of the wavelength and amplitude sensitivities (calculated from the slope of the wavelength/amplitude dependence on increasing SRI values) of modes 1 and 2 as a function of the incident polarization angle is demonstrated in Fig. 2 (c,d). Both modes show a periodical dependence of the wavelength sensitivity on the incident polarization angle (Fig. 2c), with the maximal values reaching 35-40 nm/RIU. The amplitude sensitivity (Fig. 2d) of mode 2 experiences large deviations including the sign change from negative (-794 dB/RIU) to positive (93 dB/RIU), whilst mode 1 shows smaller deviations around -300 dB/RIU. At polarization angle 0º we measure the largest wavelength shift (mode 1) and the largest amplitude shift (mode 2) possible for the current sensor configuration. It is important to note that the temperature sensitivity of all the resonances was measured after immersion of the gold-coated PCF in a bath of distilled water and increasing the temperature from 20 to 40º C. The temperature sensitivity was calculated to be 9.3 pm/ºC for the core mode, 6.9 pm/ºC for mode 1, and 7.2 pm/ºC for mode 2. The position and the power level of the fundamental Bragg resonance, as well as the difference in the temperature sensitivities, were used to compensate for the shifts of the sensing resonances due to small temperature fluctuations. The figure of merit calculated as a ratio of the wavelength sensitivity over the resonance full width at half maximum is 157 RIU^{-1} for mode 1 (for the polarization angle of 0º) which is of the same order of magnitude as for plasmonic sensors with tilted

FBGs, and higher than the values reported for other PCFs that have been considered for water refractometry so far [6]. The resolution of our PCF refractometer is 1.02×10^{-4} RIU which is comparable to the values reported for TFBGs in step-index fibers [7].

Besides tracking the shifts of a single resonance, sensitivity can also be estimated by tracking the shift of an envelope that connects several resonances from the sensing region (Fig. 3a). We applied a Matlab envelope function to the part of the transmission spectra and optimized the sampling parameter to include the modes with the largest shifts (mode 1 and 2) into the fitted spline. Modes 1 and 2 largely contribute to a shift of the envelope as a function of the increasing SRI. Fig. 3(b,c) show comparison of the sensitivities obtained from single resonance and envelope demodulation techniques. The wavelength sensitivity can be increased by ~3.6 times when the wavelength shifts of the envelope are tracked (Fig. 3b), whilst the value of the amplitude sensitivity is not improved (Fig. 3c).

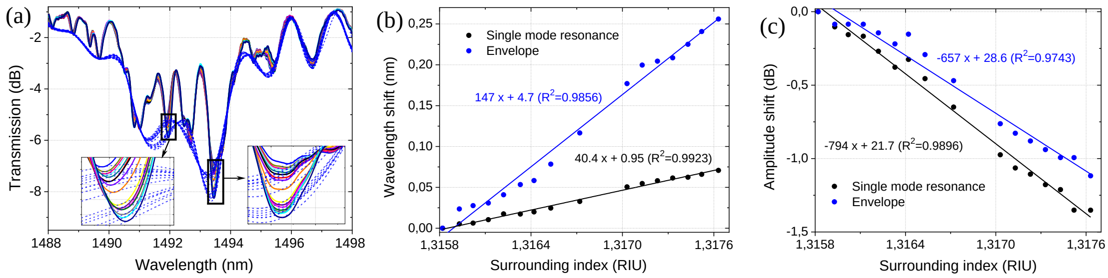

Fig. 3. **(a)** Fitting of an envelope to the transmission spectra of the gold-coated PCF sensor immersed in RI solutions. **(b,c)** Wavelength and amplitude shifts calculated after tracking a single resonance and envelope.

Conclusion

We have presented a novel type of PCF-based refractometer for measurements of aqueous solutions with cladding modes. The experimental sensitivities of 40.4 nm/RIU and -794 dB/RIU make this sensor comparable to the state-of-the-art fiber sensors and represent potential for bio-sensing applications. In addition, we demonstrated that the envelope demodulation technique allows to increase the wavelength sensitivity by ~3.6 times. The transmission spectrum shows fewer resonances than tilted FBGs in step-index fibers which shows potential for wavelength-multiplexed FBGs within a single PCF probe.

References

[1] M. Loyez *et al.*, “In situ cancer diagnosis through online plasmonics,” *Biosens. Bioelectron.*, vol. 131, no. December 2018, pp. 104–112, Apr. 2019.

[2] B. J. Eggleton, P. S. Westbrook, C. A. White, C. Kerbage, R. S. Windeler, and G. L. Burdge, “Cladding-mode-resonances in air-silica microstructure optical fibers,” *J. Light. Technol.*, vol. 18, no. 8, pp. 1084–1100, Aug. 2000.

[3] C. Chen, A. Laronche, G. Bouwmans, L. Bigot, Y. Quiquempois, and J. Albert, “Sensitivity of photonic crystal fiber modes to temperature, strain and external refractive index,” *Opt. Express*, vol. 16, no. 13, p. 9645, Jun. 2008.

[4] T. Baghdasaryan, T. Geernaert, H. Thienpont, and F. Berghmans, “Numerical modeling of femtosecond laser inscribed IR gratings in photonic crystal fibers,” *Opt. Express*, vol. 23, no. 2, p. 709, Jan. 2015.

[5] K. Chah, V. Voisin, D. Kinet, and C. Caucheteur, “Surface plasmon resonance in eccentric femtosecond-laser-induced fiber Bragg gratings,” *Opt. Lett.*, vol. 39, no. 24, p. 6887, Dec. 2014.

[6] D. J. J. Hu and H. P. Ho, “Recent advances in plasmonic photonic crystal fibers: design, fabrication and applications,” *Adv. Opt. Photonics*, vol. 9, no. 2, p. 257, Jun. 2017.

[7] J. Albert, L.-Y. Shao, and C. Caucheteur, “Tilted fiber Bragg grating sensors,” *Laser Photon. Rev.*, vol. 7, no. 1, pp. 83–108, Jan. 2013.